Supporting Information

Carboxymethyl Chitosan-Assisted Enzyme-Induced Carbonate Precipitation for Efficient Cadmium Stabilization in Contaminated Soil

Yuepeng Deng [a, 1], Jianshan Huang [a, 1], Kailu Zhang [a], Yuntao Guan[a], Lixun Zhang [a, *]

[a] Institute of Environment and Ecology, Tsinghua Shenzhen International Graduate School, Tsinghua University, Shenzhen, 518055, China

[1] These authors contributed equally to this work.

*Corresponding author: lixunz@sz.tsinghua.edu.cn.

ENGINEERING Environment

Submitted February, 2026

Method Captions

Method S1 Detailed procedures for soil column leaching experiments.

Method S2 DNA extraction, PCR amplification, and sequencing data processing.

Table Captions

Table S1 Baseline physicochemical properties of the soil prior to Cd spiking.

Table S2 Semi-quantitative elemental composition of D0 and D60 soils based on EDS analysis.

Table S3 Comparison of topological properties between empirical microbial co-occurrence networks and corresponding random networks.

Figure Captions

Fig. S1 Schematic diagram of the soil column leaching system used in this study.

Fig. S2 Effects of varying CMC addition on Cd stabilization and associated soil and solution parameters during EICP treatment.

Fig. S3 Effects of varying Urea addition on Cd stabilization and associated soil and solution parameters during EICP treatment.

Fig. S4 Temporal dynamics of soil pH, EC, and nitrogen species during EICP treatment.

Fig. S5 Differential thermal analysis (DTA) curves of EICP-remediated soil (D60) and Cd-contaminated soil amended with an equivalent amount of $CaCO_3$.

Fig. S6 Soil aggregate distribution and aggregate-associated properties at D0 and D60 following CMCS-assisted EICP remediation.

Fig. S7 Growth phenotype of P. purpureum under different treatments.

Fig. S8 SOC after correction for CMCS-derived carbon input under different treatments at 30, 60, and 90 d. Different letters indicate significant differences among treatments (one-way ANOVA followed by Duncan's multiple range test, $\alpha = 0.05$).

Fig. S9 Soil enzyme activities at D60 under different treatment.

Fig. S10 Alpha diversity of Soil under different treatment.

Fig. S11 Microbial community structure at phylum level.

Fig. S12 Microbial community structure at genus level (top 30).

Fig. S13 Phylum-level composition of nodes in microbial co-occurrence networks across different treatments

Method S1 Detailed procedures for soil column leaching experiments.

Soil column leaching experiments were conducted to evaluate cadmium (Cd) release from treated and untreated soils under controlled hydraulic and chemical conditions. The experimental design generally followed the procedure reported by Zhou et al. (Zhou et al., 2025), with modifications tailored to the present soil system. Each leaching column consisted of a cylindrical resin tube with an inner diameter of 6.25 cm and a total height of 30 cm (Fig. S1). The bottom of each column was first lined with a layer of gauze to prevent soil loss, followed by a 3 cm layer of pre-washed quartz sand (particle size 0.5–1.0 mm) to ensure uniform drainage and avoid clogging. Approximately 0.8 kg of air-dried soil was then gently filled into the column to a height of ~17 cm under gravity without mechanical compaction, resulting in a bulk density comparable to natural field conditions

Prior to leaching, all soil columns were pre-saturated from the top using the designated leaching solution at a flow rate of 50.0 mL h^{-1} to eliminate entrapped air and establish fully saturated flow conditions. The start time of the leaching experiment (t = 0) was defined as the moment when the leachate was first observed at the outlet of the column. Subsequently, continuous downward leaching was performed at operational flow rates of 6 or 12 mL h^{-1}, representing low- and high-infiltration scenarios, respectively. Two types of leaching solutions were employed: (i) simulated acid rain (pH = 3.20 ± 0.05) and (ii) near-neutral water (pH $\approx$ 6.0). The simulated acid rain solution was prepared according to the Chinese standard method HJ/T299 – 2007, using a mixed sulfuric acid and nitric acid solution at a mass ratio of 2:1, and diluted with ultrapure water to the target pH. Near-neutral leaching was conducted using untreated deionized water.

Considering laboratory constraints and the objective of capturing early-stage Cd release behavior under environmentally relevant stress conditions, the leaching experiment was conducted for a total duration of 2 days. Leachate samples were collected periodically, with each aliquot having a volume of approximately 20 mL. All

collected leachates were immediately filtered through 0.45 μm membrane filters prior to analysis.

Method S2 DNA extraction, PCR amplification, and sequencing data processing.

Microbial genomic DNA was extracted from soil samples using the E.Z.N.A.® Soil DNA Kit (Omega Bio-tek, Norcross, GA, USA) following the manufacturer's protocols. The full-length V1–V9 region of the bacterial 16S rRNA gene was amplified by PCR using the universal primers 27F (5'-AGRGTTYGATYMTGGCTCAG-3') and 1492R (5'-RGYTACCTTGTTACGACTT-3'), with unique eight-base barcodes assigned to each sample.

PCR amplification was performed in triplicate 20 μL reaction mixtures containing 4 μL of 5× FastPfu Buffer, 2 μL of 2.5 mM dNTPs, 0.8 μL of each primer (5 μM), 0.4 μL of FastPfu DNA polymerase, and approximately 10 ng of template DNA. Thermal cycling conditions consisted of an initial denaturation at 95 °C for 2 min, followed by 27 cycles of denaturation at 95 °C for 30 s, annealing at 55 °C for 30 s, and extension at 72 °C for 60 s, with a final extension at 72 °C for 5 min. PCR products were purified from 2% agarose gels using the AxyPrep DNA Gel Extraction Kit (Axygen Biosciences, Union City, CA, USA). SMRTbell libraries were constructed using the SMRTbell Prep Kit 3.0 (Pacific Biosciences) according to the manufacturer's instructions and sequenced on a PacBio Sequel IIe platform at Shanghai Biozeron Biotechnology Co., Ltd.

Raw sequencing reads were processed using the SMRT Link software to generate high-quality circular consensus sequence (CCS) reads. Sequences were filtered based on length and quality criteria, and primer and barcode sequences were removed prior to downstream analysis. High-quality sequences were clustered into operational taxonomic units (OTUs) at a defined sequence similarity threshold. Representative OTU sequences were taxonomically classified against the SILVA 16S rRNA database (SSU138.2) using a confidence threshold of 80%. OTU abundance tables were generated and rarefied to the minimum sequencing depth to minimize sampling bias before subsequent diversity and community analyses.

Table S1

Baseline physicochemical properties of the soil prior to Cd spiking.

Property	Value	Property	Value
pH	6.71	Clay (%)	0.19
EC (μs/cm)	107.21	Slit (%)	61.47
DOM (mg/kg)	29.84	Sand (%)	38.33
TN (mg/kg)	376.56	Cd (mg/kg)	0.12
CEC (cmol(+)/kg)	9.79	Ca (mg/kg)	16.50

Table S2

Semi-quantitative elemental composition of D0 and D60 soils based on EDS analysis.

Element	Atomic (%)	
	D0	D60
C	31.43	17.92
O	52.34	58.04
Si	8.28	0.70
Ca	0.09	22.58
Al	7.77	0.74
Cd	0.09	0.02

Table S3

Comparison of topological properties between empirical microbial co-occurrence networks and corresponding random networks.

	Clustering coefficient	Diameter	Modularity	Betweenness centrality
CK	0.6576	13.0014	0.4390	0.2989
CK-random	0.0920	3.9900	0.2551	0.0225
Con	0.5446	12.2082	0.6574	0.1013
Con-random	0.0408	5.0300	0.3208	0.0248
Re	0.5329	9.4053	0.5868	0.0408
Re-random	0.0430	4.4500	0.2911	0.0195

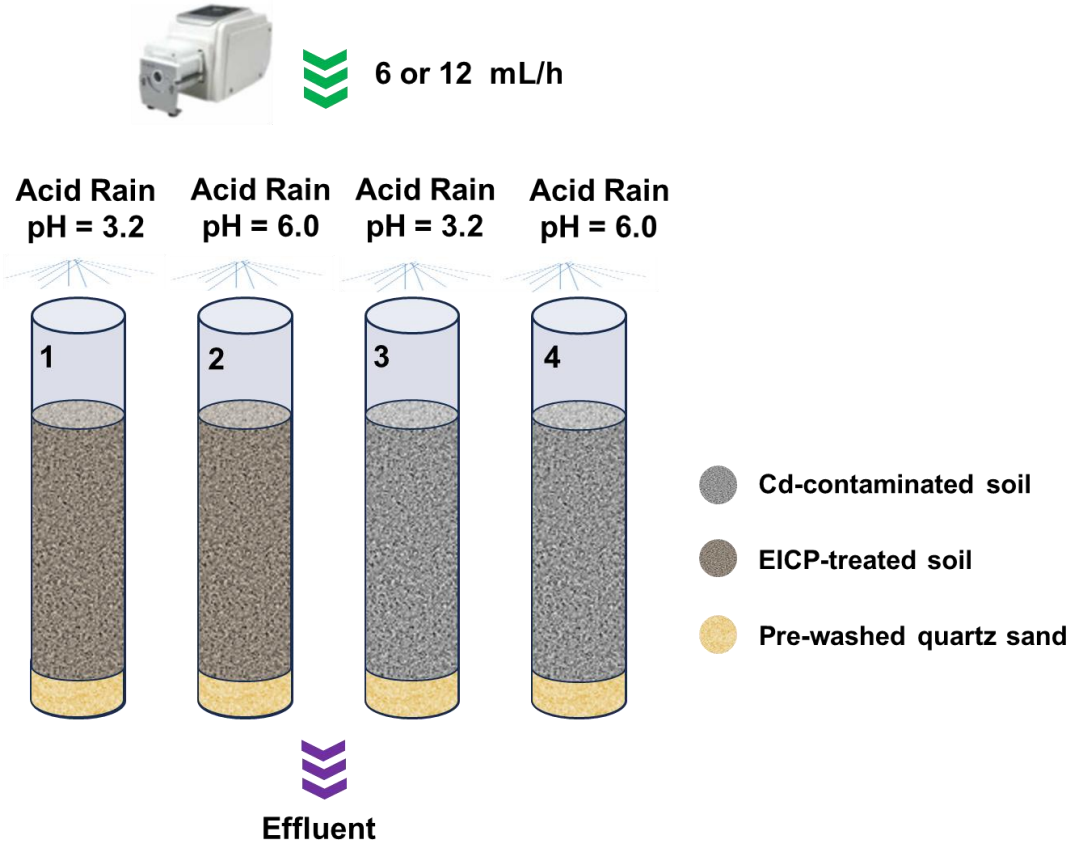

Fig. S1 Schematic diagram of the soil column leaching system used in this study.

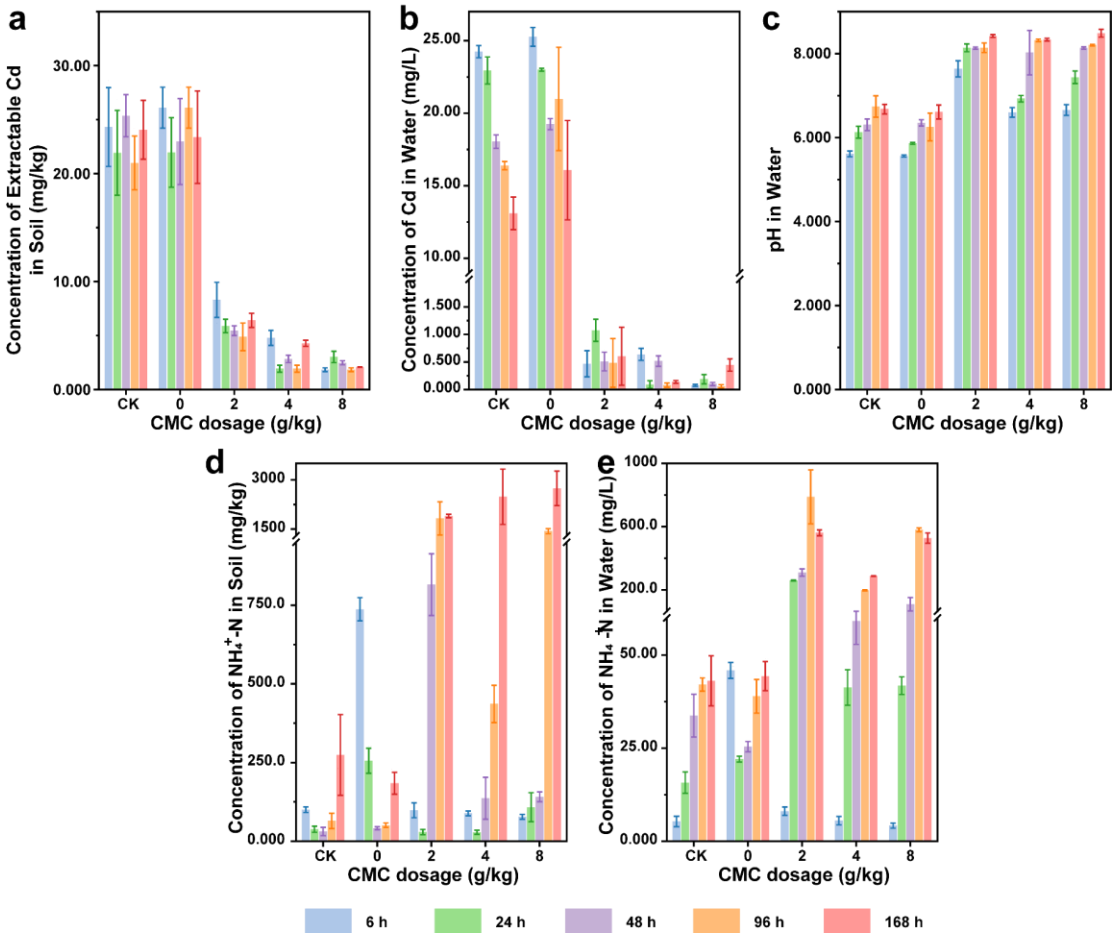

Fig. S2. Effects of varying CMC addition on Cd stabilization and associated soil and solution parameters during EICP treatment. (a) Extractable Cd concentration in soil; (b) Cd concentration in solution; (c) pH in solution; (d) NH_4^+-N concentration in soil and (e) NH_4^+-N concentration in water.

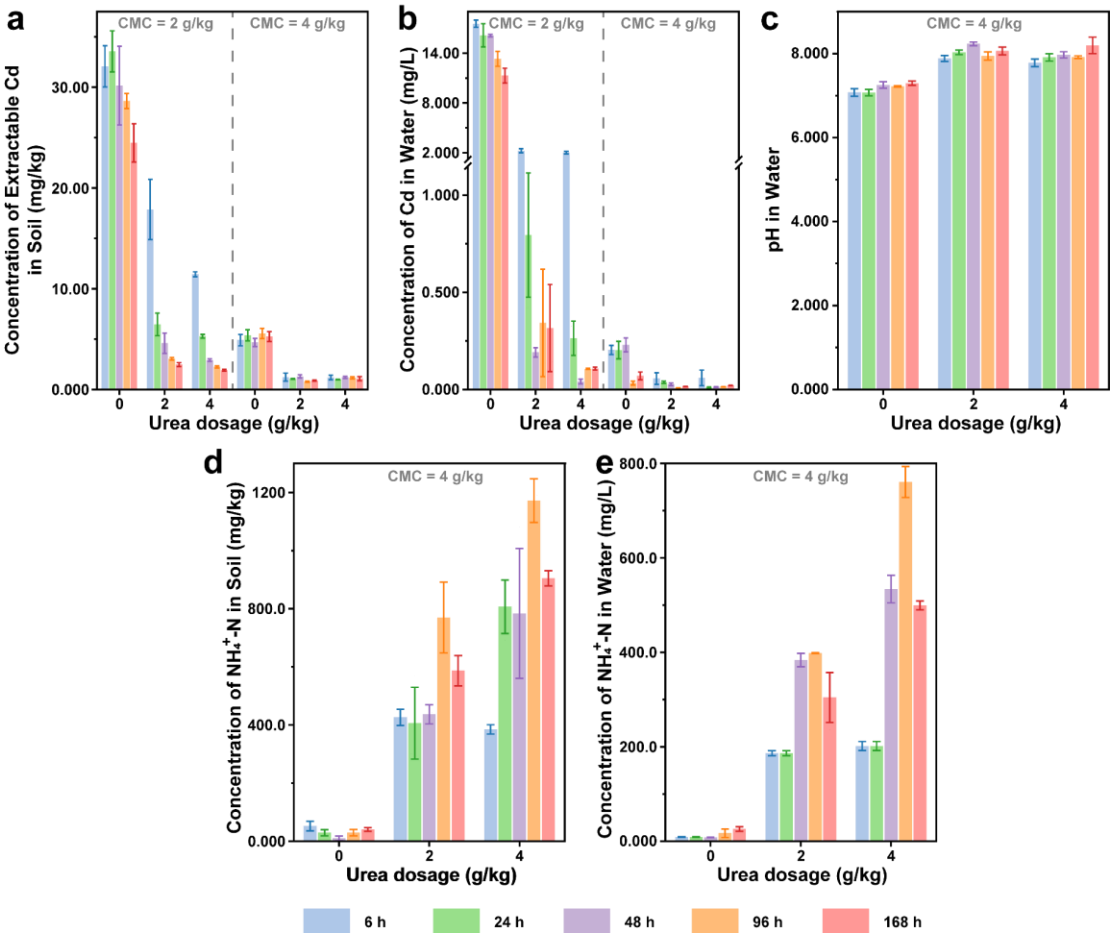

Fig. S3. Effects of varying Urea addition on Cd stabilization and associated soil and solution parameters during EICP treatment. (a) Extractable Cd concentration in soil; (b) Cd concentration in solution; (c) pH in solution; (d) NH_4^+-N concentration in soil and (e) NH_4^+-N concentration in water.

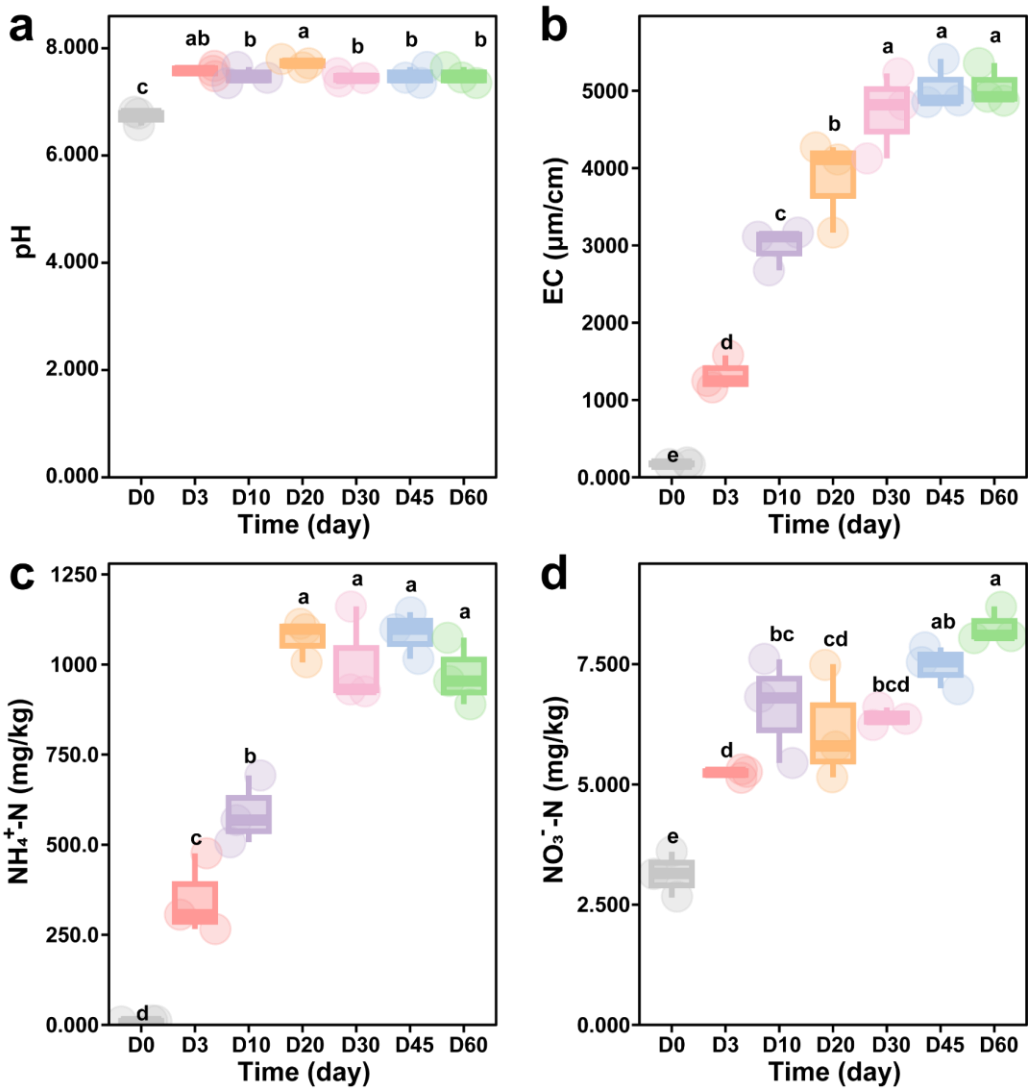

Fig. S4. Temporal dynamics of soil pH, EC, and nitrogen species during EICP treatment. (a) Soil pH; (b) EC; (c) NH_4^+-N concentration and (d) NO_3^--N concentration.

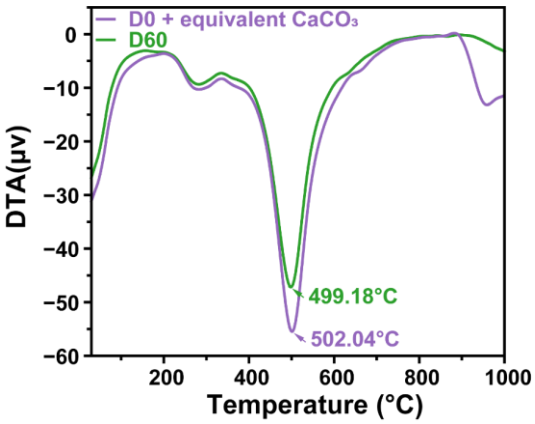

Fig. S5. Differential thermal analysis (DTA) curves of EICP-remediated soil (D60) and Cd-contaminated soil amended with an equivalent amount of $CaCO_3$.

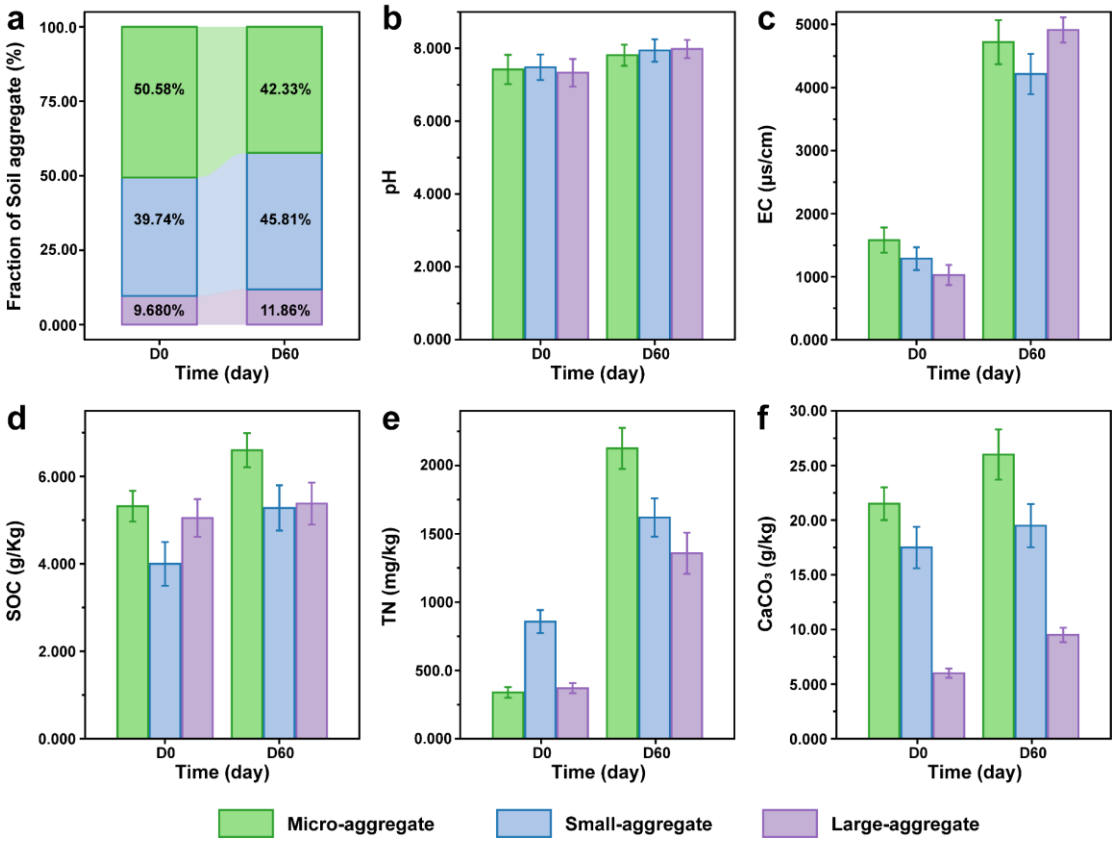

Fig. S6. Soil aggregate distribution and aggregate-associated properties at D0 and D60 following CMCS-assisted EICP remediation. (a) Proportional distribution of large aggregates, small aggregates and microaggregates fractions at D0 and D60. (b) pH of different aggregate-size fractions at D0 and D60. (c) EC of different aggregate-size fractions at D0 and D60. (d) SOC of different aggregate-size fractions at D0 and D60. (e) TN of different aggregate-size fractions at D0 and D60. (f) $CaCO_3$ associated with different aggregate-size fractions at D0 and D60.

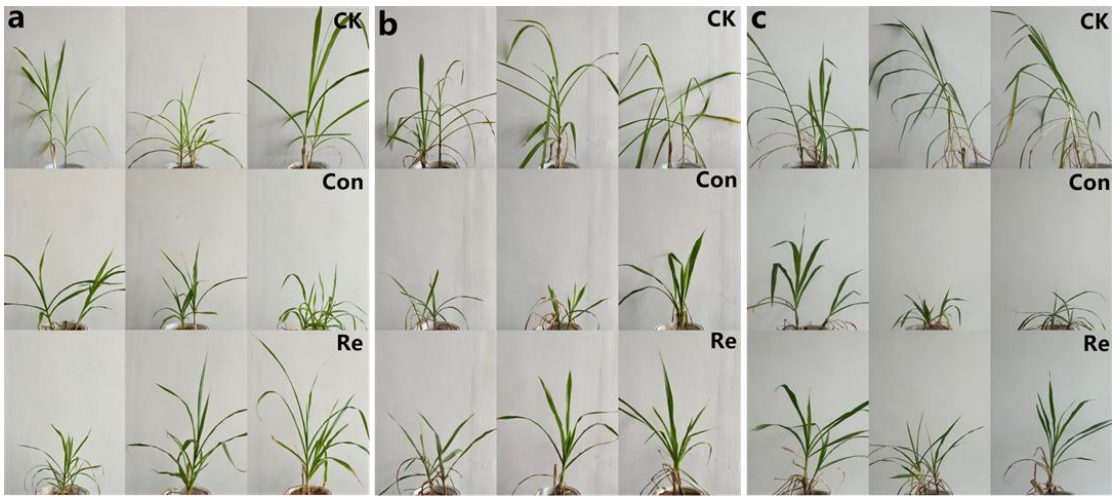

Fig. S7 Growth phenotype of *P. purpureum* under different treatments. (a) D0, (b) D45 and (c) D90.

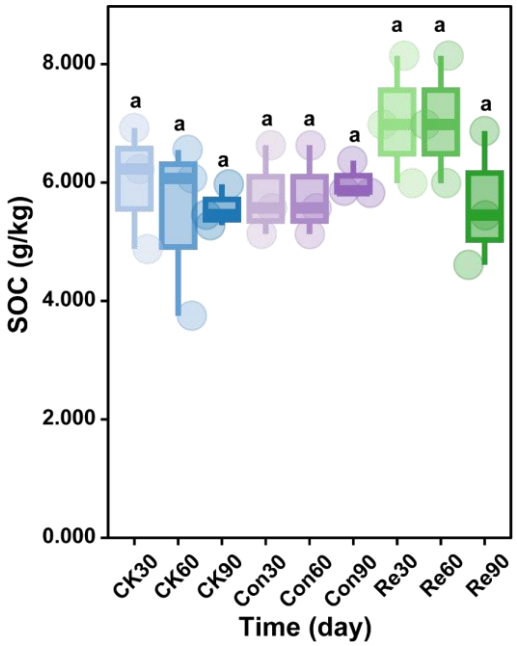

Fig. S8. SOC after correction for CMCS-derived carbon input under different treatments at 30, 60, and 90 d. Different letters indicate significant differences among treatments (one-way ANOVA followed by Duncan's multiple range test, $\alpha = 0.05$).

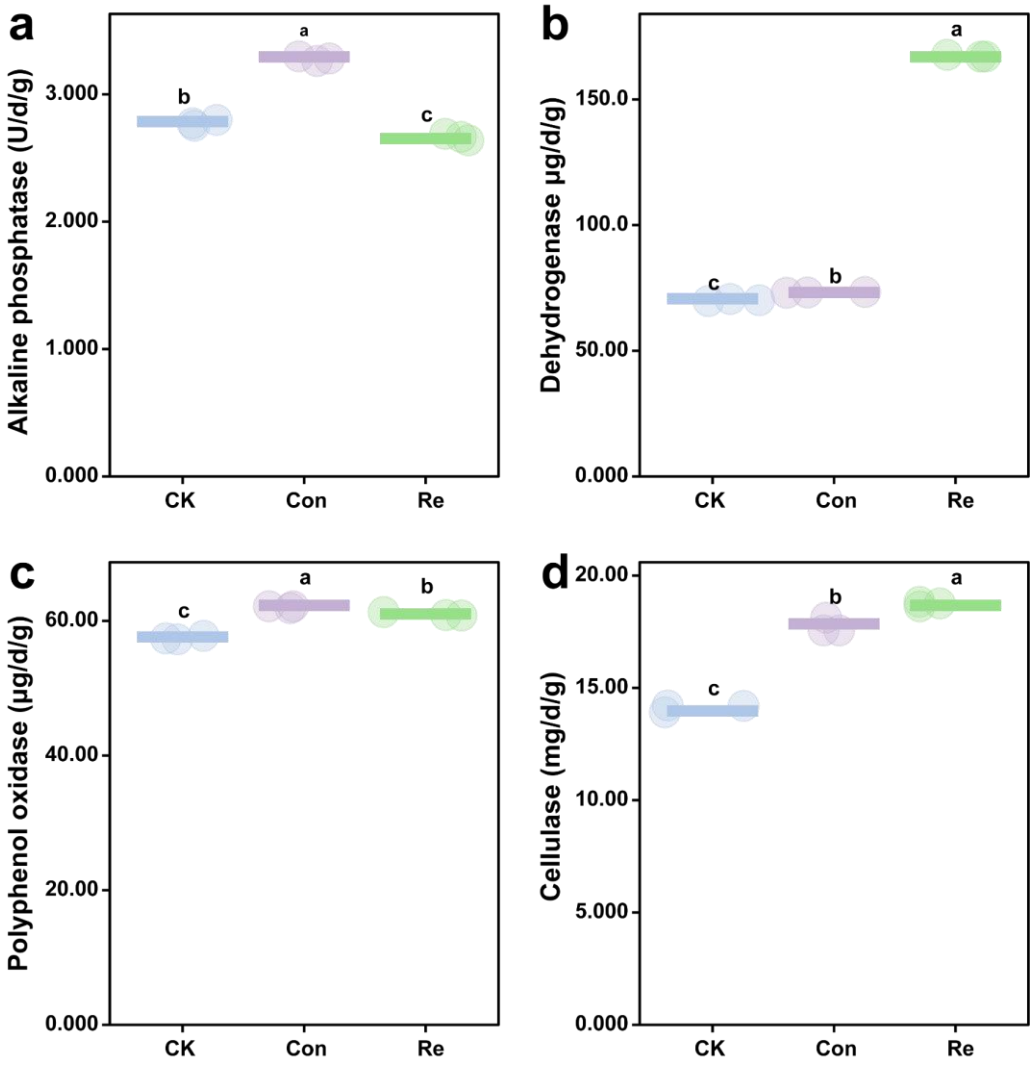

Fig. S9. Soil enzyme activities at D60 under different treatment. (a) Alkaline phosphatase activity, (b) dehydrogenase activity, (c) polyphenol oxidase activity and (d) cellulase activity.

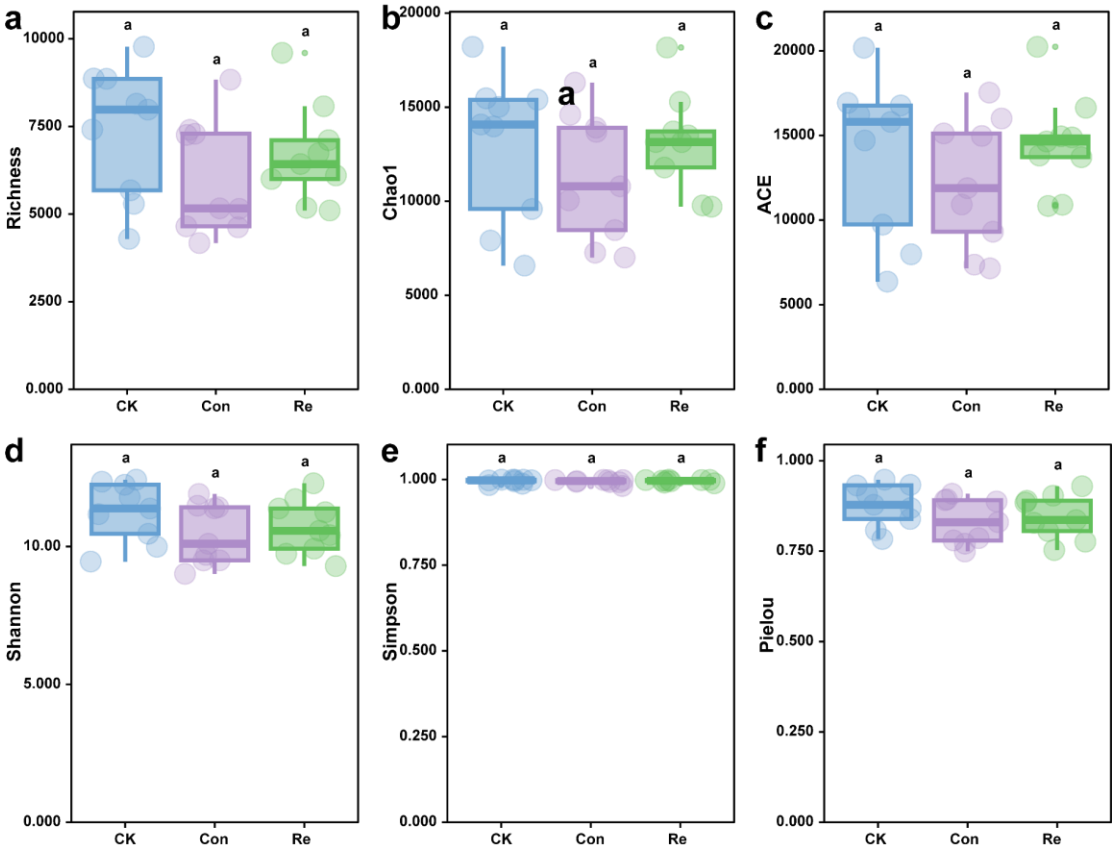

Fig. S10. Alpha diversity of Soil under different treatment. (a) Richness, (b) Chao 1, (c) ACE, (d) Shannon, (e)Simpson and (f) Pieiou.

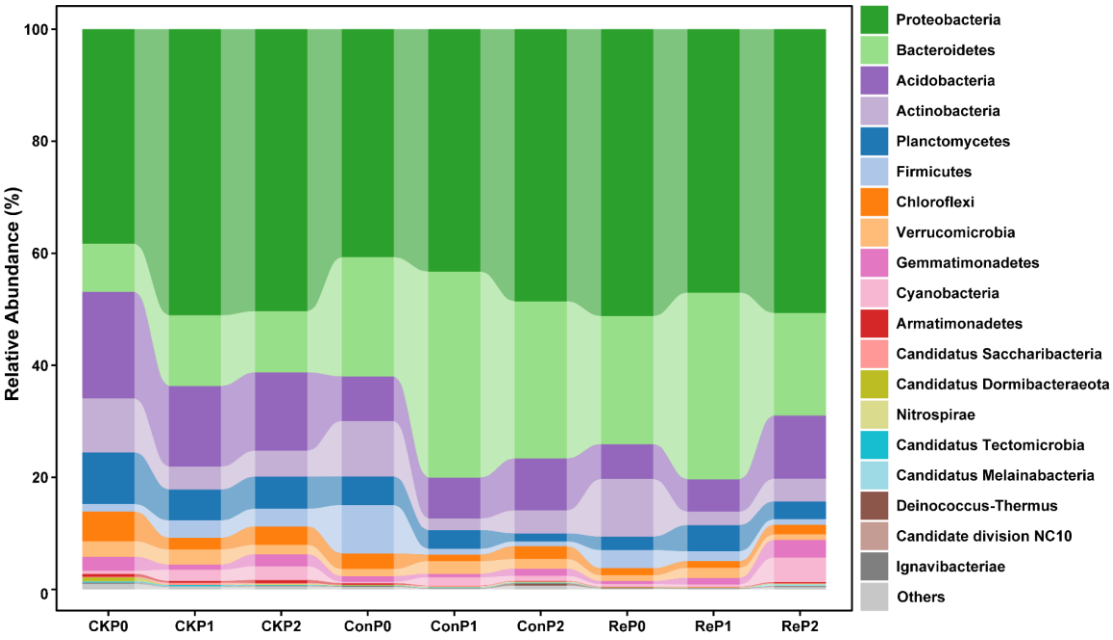

Fig. S11. Microbial community structure at phylum level.

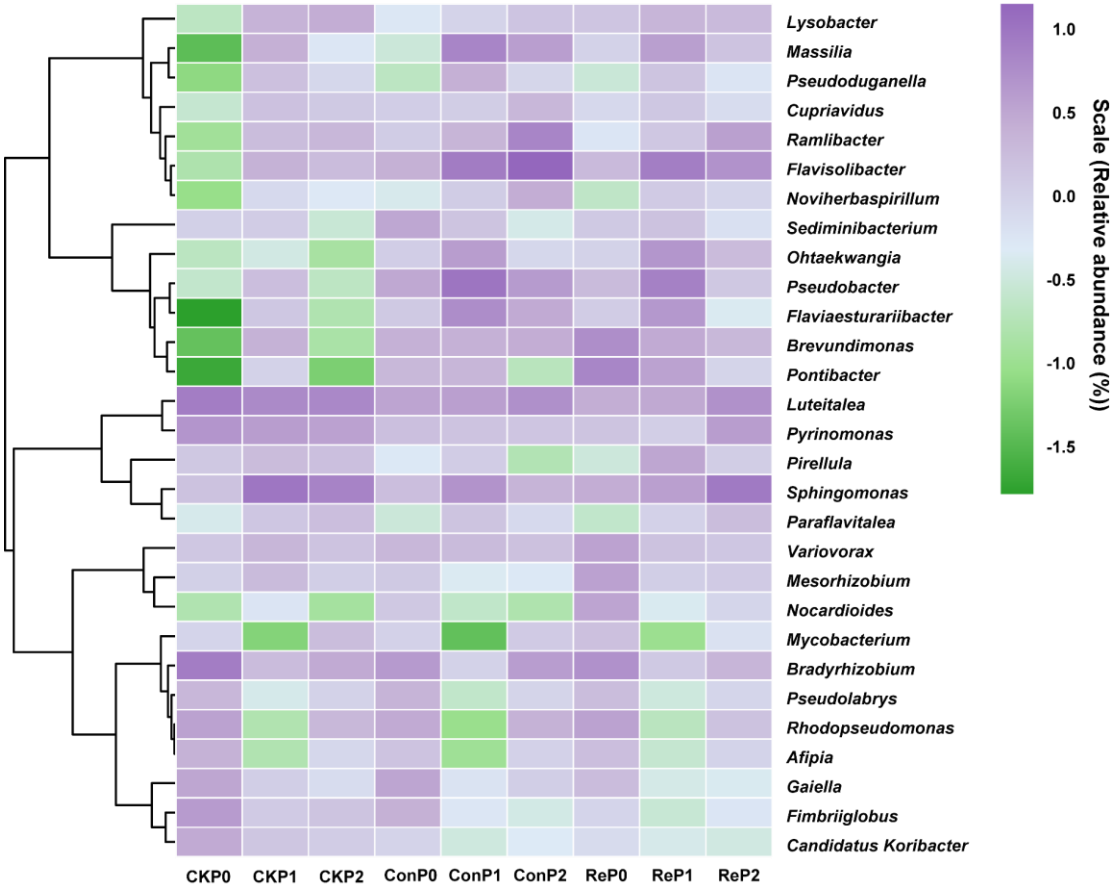

Fig. S12. Microbial community structure at genus level (top 30).

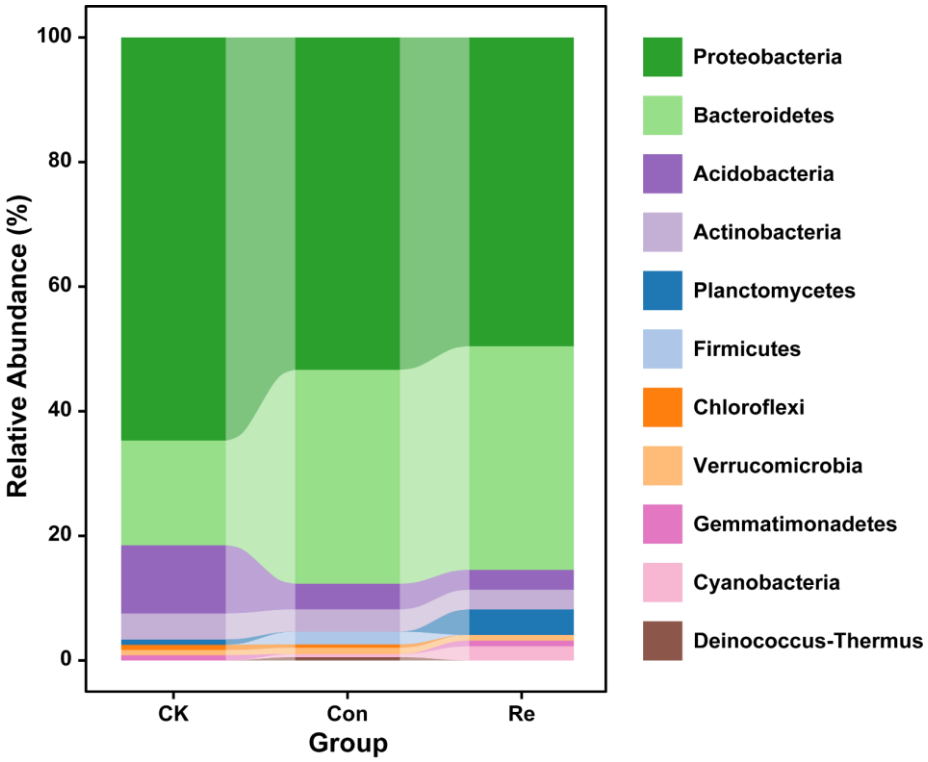

Fig. S13. Phylum-level composition of nodes in microbial co-occurrence networks across different treatments.

Supplementary Reference

Zhou J, Liu Z, Li Z, Xie R, Jiang X, Cheng J, Chen T, Yang X (2025). Heavy metals release in lead-zinc tailings: Effects of weathering and acid rain. Journal of Hazardous Materials, 483: 136645